Proceedings of the 6th WSEAS International Conference on Multimedia Systems & Signal Processing, Hangzhou, China, April 16-18, 2006 (pp31-36)

A Novel Fingerprint Algorithm Based on Line-Segment Chain[1]

DEQUN ZHAO, FEI SU and ANNI CAI
School of Telecommunication Engineering
Beijing University of Posts and Telecommunications
No.10 Xi Tu Cheng Road, Haidian District, Beijing, P.R.CHINA 100876
Peacepigeon1225@163.com

Abstract: - A novel representation of fingerprint image based on Line-Segment features which are extracted from a bank of Gabor-filtered fingerprint images is proposed in this paper. In the feature matching stage, quadrangles constructed with Perpendicularity Line-Segments are used to obtain the alignment parameters. Compared with the existing representations of fingerprint, line-Segment based representation employs not only rich discriminatory ridge information of the fingerprint images but also obviates the need for extracting minutiae points or the core point to align the fingerprint images. Experimental results show that the proposed method is robust and effective.

Key-Words: - Fingerint matching, Line-Segment, Edit-Distance, Gabor-Filter, Approximate String Matching

1 Introduction

As today's society becomes more complex, the security of information becomes more and more important. Various methods for biometric personal identification have been proposed nowadays. Among all the biometric indicators, fingerprints have one of the highest levels of reliability [1-2].

There are several practical problems in the fingerprint matching. Each time a fingerprint is acquired, location and shape distortion occur because of the elasticity of the skin [3-4]. Moreover, a high confidence and real-time matching algorithm is one of the most important stages in accurate automatic fingerprint-based identification, and it has been investigated intensively for a long time [5-9]. The widely used representation is based on minutiae such as ridge ending, and ridge bifurcation, with each minutia being characterized by its locations and orientation. Several approaches have been proposed for point pattern matching [8, 10-12], but these methods don't perform well because the minutiae-based representation does not fully utilize the discriminatory information available in fingerprint images such as ridge information, spatial properties and local structures. Considering the minutia points of a fingerprint capture only a very limited amount of information from the reachable information content present in the fingerprint pattern, Marius Tico [13] proposed an Orientation-Based Minutia Descriptor that consists of a minutia reference and a number of sampling points in a circular pattern around the minutia position. It is clear that in [13] the amount of information captured from the reachable information content present in the fingerprint pattern is still directly related to the number of minutiae and no information can be captured when there is no minutia though much reachable information content exist in these areas.

In this paper, a novel representation and matching method of fingerprint images based on Line-Segment features independent of minutia is proposed. These Line-Segment features including a rich local characterization are extracted from a bank of Gabor-filtered fingerprint images acquired by filtering the rotated fingerprints instead of using multi-channel Gabor-filtering. In the matching stage, quadrangles constructed with Perpendicularity Line-Segments are used to obtain the alignment parameters. Here, Line-Segment based representation employs rich discriminatory ridge information of the fingerprint images and what is more attractive is that it obviates the need for extracting minutiae points or the singular points used to align the fingerprint images.

The paper is organized as follows. In section2, details attendant to the Line-Segment feature extraction are described. Section 3 is dedicated for the Line-Segment pattern matching. Section 4 gives the experimental results and some discussions are presented in section 5.

2 Line-Segment feature extraction

Our proposed feature extraction algorithm is list as follows:

- Preprocessing the original gray-level fingerprint image to reduce the distortion and enhance the contrast at the same time.
- Acquiring a bank of fingerprint by rotating preprocessed fingerprint in n different directions, and then filtering the bank of rotated fingerprint images using a Gabor-filter which is tuned to a specific narrow band of spatial frequency and orientation.

[1] **Sponsored by** the National Natural Science Foundation of China (60472069)

- Thinning the bank of filtered fingerprint and constructing Line-Segment feature vectors.

2.1 Rotating and filtering

It is now widely accepted that the processing of pictorial information in the human visual system involves a set of parallel and quasi-independent mechanisms or channels [14]. It is also suggested that the receptive field profiles of many of the cortical cells—the basic elements for the hypothesized cortical channels—can well be described by Gabor functions [15]. Such psychophysical findings have led to many successful texture analysis algorithms [9, 16].

A 2D Gabor filter can be thought of as a complex plane wave modulated by a 2D Gaussian envelope. By tuning a Gabor filter to a specific frequency and direction, the local frequency and orientation information can be obtained. Thus, they are suited for extracting texture information from images [17]. The Fourier representation of the real Gabor filters is as following:

$$H(u,v;f,\theta,\delta_x,\delta_y) = C\cdot\exp\left\{-2\pi^2\cdot\left(\delta_x^2\cdot(u'-f)^2+\delta_y^2\cdot(v')^2\right)\right\} \quad (1)$$

$$u' = u\sin\theta + v\cos\theta, v' = u\cos\theta - v\sin\theta$$

where C is constant, f and θ are the radial frequency and orientation which define the location of the filters in the frequency plane, and δ_x and δ_y are the standard deviation of the Gaussian envelope along the *x* and *y* axes, respectively. Let $\Delta\theta_{1/2}$ denotes the half-band of orientation of the Gabor filter [18] which is defined as following:

$$\Delta\theta_{1/2} \approx \arctan\left(\frac{\Delta v/2}{f}\right) = \arctan\left(\frac{1}{4\sqrt{2}\pi f\delta_y}\right) \quad (2)$$

So the Gabor filter may be used to analyze the line-signal in the orientation range of ($\pi/2+\theta-\Delta\theta_{1/2}$, $\pi/2+\theta+\Delta\theta_{1/2}$).To capture entire information in a fingerprint, N_f directional-sensitive Gabor filters are needed which is obtained as follows:

$$N_f = \pi/(2\Delta\theta_{1/2}) \quad (3)$$

Traditionally, a bank of Gabor filters at various orientations is used to extract the features associated with the ridge in fingerprint [9, 19]. In our proposed method, instead of using a bank of filters, two banks of the rotated images are convolved with the $0^\circ-oriented$ Gabor filter to extract the ridge information. Convolving image with the Gabor filter in the spatial domain would be a computationally intensive operation. In order to speed-up this operation, the convolution is performed in the frequency domain. Let E_{ϕ_Q}, E_{ϕ_T} denote the rotated query and template image respectively which are defined as following:

$$E_{\phi_Q} = Rot_{\phi_Q}(E^Q); \qquad E_{\phi_T} = Rot_{\phi_T}(E^T) \quad (4)$$

where E^Q, E^T denote the query and template image respectively. $\phi_Q = i\cdot\frac{\pi}{N_Q}, i = 0,1,2,\cdots,N_Q-1$ and $\phi_T = j\cdot\frac{\pi}{N_T}, j = 0,1,2,\cdots,N_T-1$. N_Q and N_T are the number of rotated query and template images in different direction respectively. In our method, N_Q and N_T are set to 4 and 45 respectively.

In order to extract the features of the ridge at specific narrow band of spatial frequency and orientation after the Gabor filtering, the parameters $(f,\delta_x,\delta_y,\theta)$ should be set. $\delta_x = 4$, $\delta_y = 1$ and $\theta = 0^\circ$ in our algorithm based on empirical data.

Let $F=\{F_\phi\}$ denote the result of filtering on E_ϕ with the $0^\circ-oriented$ Gabor filter, where $\phi\in\{\phi_Q,\phi_T\}$.

2.2 Line-Segment Chain

2.2.1 Definitions

Since the ridge orientation typically exhibits small spatial variations between neighborhood pixels, the filtered ridge can be approximated by a relatively small number of Line-Segment (See Fig. 1 (b)).

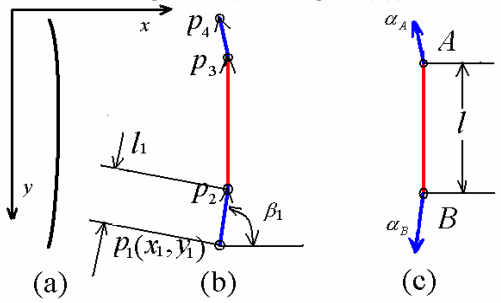

Fig.1 A Line-Segment approximation of a thinned ridge line. (a) The thinned ridge line. (b)A Line-Segment Chain consisting of 3 Line-Segments. (c) A Perpendicularity Line-Segment.

A Line-Segment can be described by a feature Vector:

$$LV=(x,y,l,\beta) \quad (5)$$

where (x,y) is its starting point coordinate, l and β are Line-Segment length and direction angle respectively. Since the filtered ridge is in the orientation range of ($\pi/2-\Delta\theta_{1/2}$, $\pi/2+\Delta\theta_{1/2}$), the range of the Line-Segment direction angle will be ($\pi/2-\Delta\theta_{1/2}$, $\pi/2+\Delta\theta_{1/2}$).

Let $LV_1(x_1,y_1,l_1,\beta_1)$ and $LV_2(x_2,y_2,l_2,\beta_2)$ denote two Line-Segments. We employ the angular d_β, the length

d_l and position cost d_p together to evaluate the dissimilarity between two Line- Segments.

The angular cost d_β of β_1 and β_2, the length cost d_l of and l_2, and the position cost d_p of $p_1(x_1, y_1)$ and $p_2(x_2, y_2)$ are described by the following equations respectively:

$$d_\beta = |\beta_1 - \beta_2| / 2\Delta\theta_{1/2} \tag{6}$$

$$d_l = \begin{cases} Tem1 / d_{l\max} & if \ \ Tem1 < d_{l\max} \\ 1 & otherwise \end{cases} \tag{7}$$

$$Tem1 = |l_1 - l_2| / \min(l_1, l_2)$$

$$d_p = \begin{cases} Tem2 / d_{p\max} & if \ \ Tem2 < d_{p\max} \\ 1 & otherwise \end{cases} \tag{8}$$

$$Tem2 = \sqrt{(x_1 - x_2)^2 + (y_1 - y_2)^2}$$

Here d_β, d_l, and d_p all take values between 0 and 1. $d_{l\max}$ is the maximum value by which two matching Line-Segments are allowed to differ in their Euclidean distances. $d_{p\max}$ is the maximum allowed difference in the Euclidean distances of two points.

A similarity function between Line-Segment is defined as:

$$S(LV_1, LV_2) = \begin{cases} \dfrac{\sqrt{d_\beta^2 + d_l^2 + d_p^2}}{3} & if \ \ d_\beta, d_l, d_p < 1 \\ 1 & otherwise \end{cases} \tag{9}$$

2.2.2 Line-Segment Chain

Our Line-Segment Chain (LSC)can be described as:

$$LSC = \{LV_i\}_{i=1}^{k} \tag{10}$$

where LV_i s are arranged in decreasing order of Y-coordinate and k denotes the number of Line-Segment in LSC . Fig.1 (b) shows a Line-Segment Chain consists of its *k* Line-Segment (here k =3).In our method, ridge information still can be captured even if there is no minutia.

Fig.2 The processing of Line-Segment approximation.

Before constructing the LSC, the ridge line will be approximated by several Line-Segments. Line-Segment approximation is processed as follows (see Fig.2).

1. Locating the starting point and ending point of the thinned ridge line;
2. Connecting the starting point and ending point with a straight line and locating the point of the thinned ridge line that has a maximum distance $D_{\max}$ to the straight line; if $D_{\max}$ is larger than a special defined threshold T_D, dividing the ridge line into two parts at the located point.

For each part of the thinned ridge line, repeat the step 1 and 2 until all $D_{\max} < T_D$.

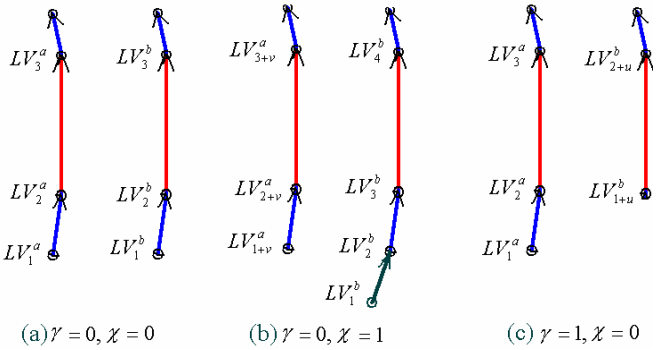

Fig.3 Illustration of determining the matched Line-Segments from two translated chains.

Let $LSC^a = \{LV_1^a, \cdots, LV_{k_a}^a\}$ and $LSC^b = \{LV_1^b, \cdots, LV_{k_b}^b\}$ denote two Line-Segment chains. k_a and k_b are the Line- Segment number of LSC^a and LSC^b respectively. For convenience, the Line-Segment chain with zero length is called the null Line-Segment chain, and it is denoted as ζ . Based on a reference Line-Segment pair which has the minimum position cost d_p^f satisfying $d_p^f < 1$, the matching relation between the Line-Segment of LSC^a and LSC^b can be determined. For two translated chains $LSC_\chi^a = \{LV_{1+\chi}^a, \cdots, LV_{k_a+\chi}^a\}$ and $LSC_\gamma^b = \{LV_{1+\gamma}^b, \cdots, LV_{k_b+\gamma}^b\}$ from LSC^a and LSC^b respectively, LV_j^a matches with LV_j^b when $j \in [1+\chi, k_a+\chi] \cap [1+\gamma, k_b+\gamma]$ (see Fig. 3). χ and γ denote the chain translation from left to right of LSC^a and LSC^b respectively are computed from the reference Line-Segment pair. χ and γ satisfy the following conditions:

$$\chi * \gamma = 0, \chi + \gamma \geq 0 \tag{11}$$

The distance function of two Line-Segment chains is defined as:

$$D(LSC^a, LSC^b) = \begin{cases} \lambda_1 + \lambda_2 + \lambda_3 & if \ \ \begin{matrix} k_a, k_b > 0 \\ and \ \ d_p^f < 1 \end{matrix} \\ k_a + k_b & if \ \ d_p^f = 1 \end{cases} \tag{12}$$

$$\lambda_1 = (\max(\chi, \gamma) - 1)$$

$$\lambda_2 = \max(k_a + \chi, k_b + \gamma) - \min(k_a + \chi, k_b + \gamma)$$

$$\lambda_3 = \sum_{j \in [1+\chi, k_a+\chi] \cap [1+\gamma, k_b+\gamma]} S(LV_j^a, LV_j^b)$$

Represent the Line-Segment Chains of rotated fingerprint images F_ϕ as a set P in the ascending order of X-coordinate of the first Line-Segment in each LSC respectively:

$P_\phi = \{LSC_1^\phi, \cdots LSC_M^\phi\}$

where M is the number of the Line-Segment chain in the rotated fingerprint image F_ϕ.

(a) Rotated image (b) Filtered image

(c) Thinned ridge map (d) Line-Segment map

Fig. 4 The results of our Line-Segment extraction algorithm on a fingerprint. (a) 0°-Rotated image in counter clockwise. (b) Filtered image by $0^\circ - oriented$ Gabor filter. (c) Thinned ridge map. (d) Line-Segment map.

From Fig.4, we can find one or more approximate Perpendicularity Line-Segment in almost all of ridges of the filtered fingerprint image. The length of the Perpendicularity Line-Segment is not the same with each other, but is changing fast even in the same fingerprint image. The Perpendicularity Line-Segment Vector PV is described as: (see Fig.1 (c))

$$PV = (x_A, y_A, \alpha_A, x_B, y_B, a_B, l)^T \quad (13)$$

where the x_*, y_* provide the locations of the Line-Segment ends in the reference frame of the print, α_* is the angle that the ridge makes with respect to the X-axis of the reference frame and l is length of Line-Segment.

3 Line-Segment matching

The two main steps in our proposed fingerprint matching based on Line-Segments involve estimating the alignment parameters using quadrangle constructed by Perpendicularity Line-Segment and aligned Line-Segment Chain Matching.

3.1 Alignment

The alignment stage is meant to recover the geometric transformation between the two fingerprint impressions in order to bring the Line-Segment feature from the query fingerprint in the spatial proximity of their corresponding counterparts from template. In our system, a revised Transformation Parameter Clustering technique of Robert's [21] is used.

The quadrangle constructed by Perpendicularity Line-Segment is used to generate key or index. The full index consists of ten components: the length of each side, the angle that the ridge or side makes with respect to the X-axis of the reference frame. l_i are the lengths of four sides. θ_1 and θ_2 is the angle of side A_1A_2 and B_2B_1 respectively. α_* is the angles of the ridges (See Fig. 5).

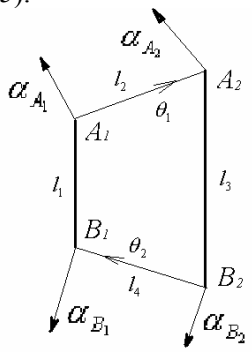

Fig.5 Illustration of Quadrangle constructed by Perpendicularity Line-Segment.

Let $Q_{\phi_Q}^Q$ and $Q_{\phi_T}^T$ denote quadrangle constructed by Perpendicularity Line-Segments from F_{ϕ_Q} and F_{ϕ_T} respectively. Using Robert's algorithm we can obtain a sorted list of hypotheses. Then the parameters of the geometric transformation, i.e., translation vector ($\mathbf{t} = [t_x, t_y]^T$) and rotation angle ($\varphi$), are calculated. The underlying assumption, justified by experimental observations, is that $\left\langle Q_{\phi_Q}^Q, Q_{\phi_T}^T \right\rangle$ is hypotheses and, hence, we have

$$\varphi = \phi_T - \phi_Q \quad (14)$$

$$\mathbf{t} = \mathbf{R}_{\phi_Q}(\mathbf{m}(c_T) - \mathbf{m}(c_Q)) \quad (15)$$

where $\mathbf{R}_\varphi$ denotes the 2×2 operator of counterclockwise rotation with φ, and c_* denotes the quadrangle center calculated by the end positions of Perpendicularity Line-Segments and the position of a point is denoted by $\mathbf{m}(*) = [x(*), y(*)]^T$.

$< P_{\phi_Q}^Q, P_{\phi_Q+\varphi}^T >$ is a corresponding pair of Line-Segment Chain set according to rotation angle φ. After translate all Line-Segment Chains of F_{ϕ_Q} by

$\mathbf{R}_{-\phi_Q}(\mathbf{t})$, the corresponding aligned Line-Segment Chains are obtained.

3.2 Aligned Line-Segment Chain Matching

Due to the existence of nonlinear deformation of fingerprints which is an inherent property of fingerprint impressions, it is impossible to exactly recover the position of each query LSC with respect to its corresponding LSC in the template. We have observed that all LSCs in the rotated fingerprint image F_ϕ can be uniquely represented by a symbol string. Therefore, the aligned Line-Segment Chain Matching can be considered as the traditional approximate string matching (ASM) problem.

For the ASM problem, there are many works have been done before. Gonzalo [22] provides a very good survey of ASM algorithms and indexing structures. A simple dynamic programming algorithm [23] can solve the problem.

Let $P^T_{\phi_T=\varphi+\phi_Q}=\{LSC^{\phi_T}_1,\cdots,LSC^{\phi_T}_{N_j}\}$ denote the set of N_j Line-Segment Chains in the template rotated fingerprint image F_{ϕ_T} and $P^{TQ}_{\phi_Q}=\{LSC^{T\phi_Q}_1,\cdots,LSC^{T\phi_Q}_{M_i}\}$ denote the set of M_i Line-Segment Chains in the query rotated fingerprint image F_{ϕ_Q} which is aligned with the above template according to translation vector $\mathbf{t}$. Further, the Line-Segment Chains are denoted as the symbols and we use the strings $\mathbf{s}=s_1s_2\cdots s_{N_j}$ and $\mathbf{q}=q_1q_2\cdots q_{M_i}$ to represent the template and query rotated fingerprint image, respectively.

Given two strings $\mathbf{q}$ and $\mathbf{s}$ of length M_i and N_j respectively, the edit cost function $C_{m,n}$, in our algorithm is defined with the following equation:

$$C_{0,0}=0$$

$$C_{m,n}=\min\begin{Bmatrix} C_{m-1,n-1}+\delta(q_m,s_n) \\ C_{m-1,n}+\delta(q_m,\varepsilon) \\ C_{m,n-1}+\delta(\varepsilon,s_n) \end{Bmatrix} \begin{matrix} 0<m\le M_i \\ and \\ 0<n\le N_j \end{matrix} \quad (16)$$

where $\delta(q_m,s_n)=D(LSC^{\phi_T}_m,LSC^{T\phi_Q}_n)$, $\delta(q_m,\varepsilon)=D(LSC^{\phi_T}_m,\zeta)$ and $\delta(\varepsilon,s_n)=D(\zeta,LSC^{T\phi_Q}_n)$.

Then we construct the edit graph G associated with $\mathbf{q}$ and $\mathbf{s}$ to find the shortest path from the left upper corner to the right-down corner [24]. By tracing the minimum cost edit sequence, the matching relation between the Line-Segment chain of $\mathbf{q}$ and $\mathbf{s}$ can be determined. And the similarity S_{QT} between the query and template fingerprints is then computed according to the following formula:

$$S_{QT}=(1-\frac{1}{N_Q}\sum_{\phi_Q\in\left\{i\cdot\frac{\pi}{N_Q}\mid\ i=0,1,2,\cdots,N_Q-1\right\}}(C^{\phi_Q}_{M_i,N_j})/L_{\phi_Q}) \quad (17)$$

where L_{ϕ_Q} denotes the total number of Line-Segment in $P^{TQ}_{\phi_Q}$ and $P^T_{\phi_T=\varphi+\phi_Q}$. The maximum and minimum values of the similarity S_{QT} are 1 and 0, respectively. The former value indicates a perfect match, while the later value indicates no match at all.

4 Experimental Results

In order to evaluate the performance of our proposed algorithm, the matching method described above was tested with FVC2002 DB2 set A. The set contains 800 fingerprint images captured at a resolution of 569 dpi, from 100 fingers (eight impressions per finger). The size of the images is 296×560.

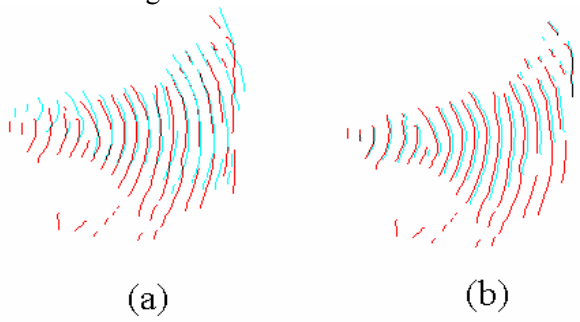

Fig.6 Illustration of alignment of thinned fingerprint images based on quadrangle. (a) Two thinned images from different finger. (b) Two thinned images from the same finger.

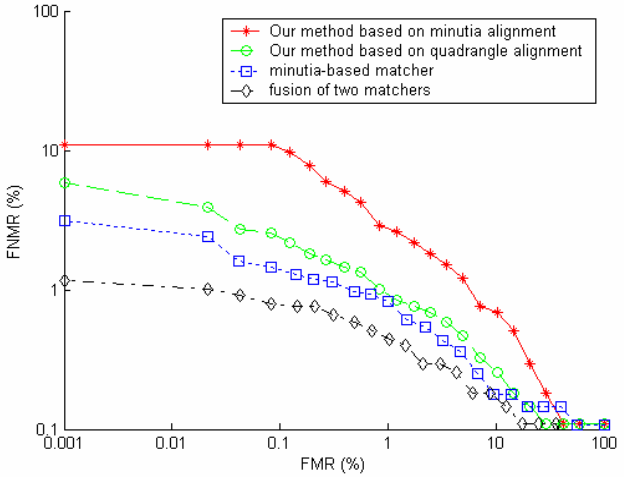

Fig.7 The ROC curves depicting matching performance

An example of the alignment of thinned images using our algorithm has been illustrated (see Fig.6). Fig.7 shows the difference Receiver Operating Characteristic (ROC) curves by plotting the False Non Match Rate (FNMR) vs. the False Match Rate (FMR) for the database. From our experiments, alignment based on quadrangle has the advantage over that based on minutia when the number of minutiae in overlap between two fingerprint images is small (such as less

than 20). The comparison of the proposed technique with the minutia-based matcher is given by plotting the ROC of the matching score. From Fig. 7, we can see that the minutia-based matcher demonstrates a better performance than the Line-Segment based matcher and the fusing of two matchers (by normalizing and adding the matching scores) results in an improved performance of the fingerprint verification system.

5 Conclusions

This work elucidates a novel fingerprint matching technique that employs an efficient quadrangle and Line-Segment feature to align and match fingerprint images respectively. The quadrangles obviate the need to use the minutiae or core information to align image pairs. The quadrangles also can provide more information to align image pairs than minutiae when the overlap between two fingerprint images is small. It must be mentioned here the performance of the proposed technique is inferior to that of a minutiae-based fingerprint matcher at the present. However, when used alongside a minutiae matcher, an improvement in matching performance is observed. Currently we are looking into the ways to extract Line-Segment feature of low quality fingerprint images with less errors.

References:

[1] John Berry and David A. Stoney, "The history and development of fingerprinting," in *Advances in fingerprint Technology*, Henry C. Lee and R.E. Gaensslen, Eds., pp. 1–40. CRC Press, Florida, 2nd edition, 2001.

[2] Emma Newham, "The biometric report," *SJB Services*, 1995.

[3] Coetzee, L. and Botha, E. C. Fingerprint recognition in low quality images, *Pattern Recognition*, 26(10):1441–1460, Oct. 1993.

[4] Wilson, C. L., Candela, G. T. and Watson, C. I. Neural-network fingerprint classification, *J. Artificial Neural Networks*, 1(2):203–228, Feb. 1994.

[5] Rao, A. R. and Balk, K. Type classification of fingerprints: A syntactic approach, *IEEE Transactions on Pattern Analysis and Machine Intelligence*, PAMI-2(3):223–231, Mar. 1980.

[6] M. Eshera and K. S. Fu, "A similarity measure between attributed relational graphs for image analysis," *in Proc. 7th Int. Conf. Pattern Recognition, Montreal, P.Q., Canada*, July 30–Aug. 3 1984.

[7] S. Gold and A. Rangarajan, "A graduated assignment algorithm for graph matching," *IEEE Trans. Pattern Anal. Machine Intell.*, vol. 18, no. 4, pp. 377–388, 1996.

[8] A. K. Jain, L. Hong, S. Pankanti, and R. Bolle, "An identity authentication system using fingerprints," *Proc. IEEE*, vol. 85, pp. 1365–1388, Sept. 1997.

[9] A. K. Jain, S. Prabhakar, L. Hong, and S. Pankanti, "Filterbank-based fingerprint matching," *IEEE transactions on Image Processing*, vol. 9, pp. 846-859, May 2000.

[10] A. Ranade, A. Rosenfeld, "Point Pattern Matching by Relaxation", *Pattern Recognition*, Vol. 26, No. 2, pp.269-276, 1993.

[11] J. P. P. Starink, E. Backer, "Finding Point Correspondence Using Simulated Annealing", *Pattern Recognition*, Vol. 28,No.2, pp. 231-240, 1995.

[12] Li Hua Zhang, WenLi Xu, "Point Pattern Matching",*Chinese Journal of Computer Science*, Vol. 22, No. 7,1999.

[13] Marius Tico, and Pauli Kuosmanen, "Fingerprint Matching Using an Orientation-Based Minutia Descriptor", *IEEE Transactions On Pattern Analysis And Machine Intelligence*, VOL. 25, NO. 8, AUGUST 2003, pp 1009-1014.

[14] D.A. Pollen and S.F. Ronner, "Visual Cortical Neurons as Localized Spatial Frequency Filters," *IEEE Trans. Systems, Man, and Cybernetics, vol. 13,* pp. 907-916, 1983.

[15] J.G. Daugman, "Uncertainty Relation for Resolution in Space, Spatial Frequency, and Orientation Optimized by 2D Visual Cortical Filters," *J. Optical Soc. Am. A, vol. 2,* pp. 1,160-1,169, 1985.

[16] Arun Ross, James Reisman and Anil Jain,Appeared, "Fingerprint Matching Using Feature Space Correlation," *Proc. of Post-ECCV Workshop on Biometric Authentication, LNCS 2359*, pp.48-57, Denmark, June 1, 2002.

[17] Arun Rossa, Anil Jaina, James Reismanb, "A hybrid fingerprint matcher," *Pattern Recognition* 36 1661-1673, 2003.

[18] J.G. Daugman, "Uncertainly relation for resolution in space, spatial frequency, and orientation optimized by two-dimensional visual cortical filters", *Journal of the Optical Society of America (A)*, vol 2(7), pp. 1160-1169, 1985.

[19] A. K. Jain, A. Ross, and S. Prabhakar, "Fingerprint matching using minutiae and texture features, " *in Proc. International Conference on Image Processing (ICIP), (Thessaloniki, Greece),* pp. 282-285, Oct 2001.

[20] L. Hong, Y. Wan, A.K. Jain, "Fingerprint image enhancement: Algorithms and performance evaluation," *IEEE Trans. Pattern Anal. Mach. Intell.* , Vol. 20, NO. 8, 777–789, 1998.

[21] Robert S., Andera, And Scott Colville, "Fingerprint Matching Using Transformation Parameter Clustering", *IEEE Computational Science & Engineering*, 1997, PP 42-49.

[22] Gonzalo Navarro, "A Guided Tour to Approximate String Matching", *ACM Computing Surveys, Vol. 33, No. 1,* March 2001, pp. 31–88.

[23] Sellers, "The theory and computation of evolutionary distances", *Pattern recognition. J. Algor. 1,* 1980, pp.359–373.

[24] R. A. Wagner and M. J. Fischer, "The string-to-string correction problem," *J. ACM, vol. 21,* pp. 168–173, 1974